Available online at www.sciencedirect.com
ScienceDirect
Mathematical Biosciences 210 (2007) 335–354
Mathematical Biosciences
www.elsevier.com/locate/mbs

Effects of density-dependent migrations on stability of a two-patch predator–prey model

Abderrahim El Abdllaoui [a], Pierre Auger [a,*], Bob W. Kooi [b], Rafael Bravo de la Parra [c], Rachid Mchich [d]

[a] *IRD, Institut de Recherche pour le Développement, U. R. GEODES, Centre de Recherche d'Ile de France, 32 Avenue Henri Varagnat, 93143 Bondy cedex, France*
[b] *Department of Theoretical Biology, Institute of Ecological Science, Vrije Universiteit, De Boelelaan 1087, 1081 HV Amsterdam, The Netherlands*
[c] *Departamento de Matemáticas, Universidad de Alcalá, 28871 Alcalá de Henares, Madrid, Spain*
[d] *Ecole Nationale de Commerce et de Gestion, B.P. 1255, 90000 Tanger, Morocco*

Received 20 November 2006; received in revised form 5 March 2007; accepted 9 March 2007
Available online 18 March 2007

Abstract

We consider a predator–prey model in a two-patch environment and assume that migration between patches is faster than prey growth, predator mortality and predator–prey interactions. Prey (resp. predator) migration rates are considered to be predator (resp. prey) density-dependent. Prey leave a patch at a migration rate proportional to the local predator density. Predators leave a patch at a migration rate inversely proportional to local prey population density. Taking advantage of the two different time scales, we use aggregation methods to obtain a reduced (aggregated) model governing the total prey and predator densities. First, we show that for a large class of density-dependent migration rules for predators and prey there exists a unique and stable equilibrium for migration. Second, a numerical bifurcation analysis is presented. We show that bifurcation diagrams obtained from the complete and aggregated models are consistent with each other for reasonable values of the ratio between the two time scales, fast for migration and slow for local demography. Our results show that, under some particular conditions, the density dependence of

* Corresponding author.
E-mail addresses: elabdll@bondy.ird.fr (A.E. Abdllaoui), pierre.auger@bondy.ird.fr (P. Auger), kooi@bio.vu.nl (B.W. Kooi), rafael.bravo@uah.es (R.B. de la Parra), racmchich@yahoo.com (R. Mchich).

0025-5564/$ - see front matter
doi:10.1016/j.mbs.2007.03.002

migrations can generate a limit cycle. Also a co-dim two Bautin bifurcation point is observed in some range of migration parameters and this implies that bistability of an equilibrium and limit cycle is possible.

Keywords: Aggregation methods; Bifurcation analysis; Density-dependent migrations; Community stability; Spatial predator–prey model

1. Introduction

In their review on spatial predator–prey models [1], Briggs and Hoopes classify these models by reaction-diffusion, individual based and patch (global migration) and lattice (migration only with local neighbour patches) models. In this work, we consider a predator–prey model in a system of two patches connected by migrations. The main goal of this work is to study the effects of density-dependent migrations on the dynamics of the predator–prey system. We assume that prey leave faster a given patch the more predators are there at that time. Similarly, we suppose that the more prey stay in a patch the slower predators would move to the other patch where the prey density is unknown and may be small. In two previous contributions, with a similar setting, we investigated separately the effects of prey density-dependent migration of predators [2], and of predator density-dependent prey migration [3] on the dynamics of a two-patch predator prey system. In this work, we study the coupling of the two kinds of density-dependent migrations.

The interaction between local dynamics, changes over time in births and deaths within each local community, and dispersal, migrations from one patch to another in an heterogeneous environment, has important consequences for community stability. Theory tells us that population persistence in patchy environments results from an interaction between local interactions, dispersal and spatial heterogeneity [4,5]. Despite empirical evidence (see [4] and references there in), few theoretical studies have addressed the effects of density-dependent dispersal. We could, nevertheless, cite the following ones: [6–11]. On another aspect of the subject, most works consider dispersal and local interactions taking place at the same time scale; we have found, apart from [2,3], only in [12] that dispersal is assumed to occur at a fast time scale, though this might be the case in many situations.

The inclusion of two time scales in the system has the advantage of allowing the reduction of the system which may become, in this way, mathematically more tractable. Otherwise, taking into account several patches and density-dependent migrations may lead to models so complex that only few general results can be obtained analytically. The reduction of the proposed system is undertaken with the help of aggregation methods which aim at studying the relationships between a large class of complex systems, in which many variables are involved, and their corresponding reduced or aggregated systems, governed by a few variables. Perfect and approximate aggregation in population dynamics were introduced in [13,14]. The kind of aggregation methods to be used in this work is based on time scale separation methods. For such methods we refer to [15–18]. Several applications of these aggregation methods in population and community dynamics can be found in [19–23].

The article is organized as follows. In Section 2, we present a general two-patch predator prey model with density-dependent migrations. There, for a large class of density-dependent migration

rules for prey and predators, we show that migration attaints a unique positive and stable equilibrium for each fixed values of the prey and predators global densities. This fact together with the existence of two time scales allow us to use time scale separation methods, leading to the construction of a reduced or 'aggregated' model governing the total prey and predator densities. In Section 3, we treat a particular case of the system presented in Section 2 with prey migration rates linearly depending on predator local density and with predator migration rates inversely proportional to prey local density. We perform numerical bifurcation analysis of the complete and aggregated models to help in the study of the effects of density-dependent migrations on the stability of the predator–prey system and in the light of that we revisit some earlier contributions. Section 4 is devoted to a discussion and conclusions.

2. A general two-patch predator–prey model with predator density-dependent migration of prey and prey density-dependent migration of predators and fast migration

2.1. The complete model

In this section, we present a general model of a two-patch predator–prey system. The patches are connected by migrations while locally there is a predator–prey interaction. We assume that migrations occur at a fast time scale in comparison with the local predator–prey dynamics. Parameter ε, small and dimensionless, represents the ratio of fast to slow time scales. The complete predator prey model reads as follows:

$$\begin{cases} \frac{dn_1}{d\tau} = f_2(p_2)n_2 - f_1(p_1)n_1 + \varepsilon\left[\phi_1(n_1)n_1 - \widetilde{\phi}_1(n_1)p_1\right] \\ \frac{dn_2}{d\tau} = f_1(p_1)n_1 - f_2(p_2)n_2 + \varepsilon\left[\phi_2(n_2)n_2 - \widetilde{\phi}_2(n_2)p_2\right] \\ \frac{dp_1}{d\tau} = g_2(n_2)p_2 - g_1(n_1)p_1 + \varepsilon\left[-\psi_1(p_1) + \widetilde{\psi}_1(n_1)p_1\right] \\ \frac{dp_2}{d\tau} = g_1(n_1)p_1 - g_2(n_2)p_2 + \varepsilon\left[-\psi_2(p_2) + \widetilde{\psi}_2(n_2)p_2\right] \end{cases} \tag{1}$$

where τ is the fast time scale and then $t = \varepsilon\tau$ the slow time scale. Prey densities on patch 1 and 2 are, respectively, denoted n_1 and n_2; the corresponding predator densities are p_1 and p_2.

Hypotheses. Functions f_i, $i = 1,2$, are $C^1(\mathbb{R}_+)$, increasing and satisfy $f_i(x) > 0$ for $x > 0$, and functions g_i, $i = 1,2$, are $C^1(\mathbb{R}_+)$, decreasing and satisfy $g_i(x) > 0$ for $x > 0$.

Functions $f_1(p_1)$ and $f_2(p_2)$ represent prey migration rates from patch 1 to patch 2, resp. from patch 2 to patch 1, and are assumed to depend on the corresponding predator local density. We further assume that these functions are monotonically increasing with predator density describing the fact that the more predators are located in a patch the more likely prey leave it.

Functions $g_1(n_1)$ and $g_2(n_2)$ are predator migration rates from patch 1 to patch 2, resp. from patch 2 to patch 1, and are assumed to be prey local density-dependent. Consequently, we also assume that they are monotonically decreasing with prey density which reflects that predators are more likely to remain in a patch where in the prey density increases.

Functions $\phi_1(n_1)$ and $\phi_2(n_2)$ are per capita prey growth rates on each patch. Similarly, $\psi_1(p_1)$ and $\psi_2(p_2)$ are predator mortality rates in absence of prey. The functional responses on each patch are $\widetilde{\phi}_1(n_1)$ and $\widetilde{\phi}_2(n_2)$ while $\widetilde{\psi}_1(n_1)$ and $\widetilde{\psi}_2(n_2)$ are predator per capita growth rates due to predation.

As the complete model involves two time scales, we are going to use aggregation methods in order to build a reduced model governing the total prey and predator densities. First, we study the fast system of (1), then we give the aggregated model associated.

2.2. Fast system

The fast model is obtained by neglecting the slow dynamics, i.e. taking $\varepsilon = 0$

$$\begin{cases} \frac{dn_1}{d\tau} = f_2(p_2)n_2 - f_1(p_1)n_1 \\ \frac{dn_2}{d\tau} = f_1(p_1)n_1 - f_2(p_2)n_2 \\ \frac{dp_1}{d\tau} = g_2(n_2)p_2 - g_1(n_1)p_1 \\ \frac{dp_1}{d\tau} = g_1(n_1)p_1 - g_2(n_2)p_2 \end{cases} \tag{2}$$

Denoting $n = n_1 + n_2$ the total prey density and $p = p_1 + p_2$ the total predator density we see that they are both constants of motion of system (2), so the study of the existence of fast equilibria and their stability can be carried out for the next system

$$\begin{cases} \frac{dn_1}{d\tau} = f_2(p - p_1)(n - n_1) - f_1(p_1)n_1 \\ \frac{dp_1}{d\tau} = g_2(n - n_1)(p - p_1) - g_1(n_1)p_1 \end{cases} \tag{3}$$

where we suppose that n and p are two positive constants and we have done the following substitutions: $n_2 = n - n_1$ and $p_2 = p - p_1$. Fast equilibria satisfy the following system:

$$\begin{cases} (n - n_1)f_2(p - p_1) = f_1(p_1)n_1 \\ (p - p_1)g_2(n - n_1) = g_1(n_1)p_1 \end{cases} \tag{4}$$

which is equivalent to

$$\begin{cases} n_1 = \frac{nf_2(p-p_1)}{f_1(p_1)+f_2(p-p_1)} \\ p_1 = \frac{pg_2(n-n_1)}{g_1(n_1)+g_2(n-n_1)} \end{cases} \tag{5}$$

Denoting

$$h(x) = \frac{nf_2(p - x)}{f_1(x) + f_2(p - x)} \quad \text{and} \quad \widetilde{h}(x) = \frac{pg_2(n - x)}{g_1(x) + g_2(n - x)} \tag{6}$$

system (5) implies that

$$p_1 = \widetilde{h}(h(p_1)) \tag{7}$$

Remark here that the functions h and $\widetilde{h}$ are continuous and positive in $]0, p[$ and $]0, n[$, respectively. Moreover, we have

$$h'(x) = -\frac{nf_1(x)f_2'(p-x) + nf_2(p-x)f_1'(x)}{(f_1(x)+f_2(p-x))^2}$$
$$\widetilde{h}'(x) = -\frac{pg_1(x)g_2'(n-x) + pg_2(n-x)g_1'(x)}{(g_1(x)+g_2(n-x))^2}$$

The hypotheses on functions f_i and g_i make function h decreasing and function $\widetilde{h}$ increasing, which implies that $\widetilde{h} \circ h$ is decreasing. Consequently, if a solution of (7) exists, it will be unique. Besides we have that $h(]0,p[) \subset]0,n[$ and $\tilde{h}(]0,n[) \subset]0,p[$, which yields

$$\tilde{h} \circ h(]0,p[) \subset]0,p[$$

and thus there exists a unique positive $p_1^* \in]0,p[$ such that

$$p_1^* = (\widetilde{h} \circ h)(p_1^*)$$

with the corresponding n_1 value: $n_1^* = \frac{nf_2(p-p_1^*)}{f_1(p_1^*)+f_2(p-p_1^*)}$

As for each pair (n,p) there exists a unique equilibrium (n_1^*, p_1^*) of system (3), we denote

$$\begin{aligned} &n_1^* = n_1^*(n,p) \quad \text{and} \quad p_1^* = p_1^*(n,p) \\ &n_2^* = n_2^*(n,p) = n - n_1^*(n,p) \quad \text{and} \quad p_2^* = p_2^*(n,p) = p - p_1^*(n,p) \end{aligned} \tag{8}$$

Let us now study the stability of (n_1^*, p_1^*) for system (3). It is easy to see that the Jacobian matrix evaluated at the equilibrium is given by

$$J = \begin{pmatrix} -f_2(p-p_1^*) - f_1(p_1^*) & -(n-n_1^*)f_2'(p-p_1^*) - n_1^* f_1'(p_1^*) \\ -(p-p_1^*)g_2'(n-n_1^*) - p_1^* g_1'(n_1^*) & -g_2(n-n_1^*) - g_1(n_1^*) \end{pmatrix}$$

Therefore, using the fact that functions f_i are positive and increasing and functions g_i are positive and decreasing, we obtain $\mathrm{Det}(J) > 0$ and $\mathrm{Tr}(J) < 0$, which implies that the fast equilibrium is stable.

The aggregated model for the global variables n and p, expressed in terms of the slow time scale $t = \varepsilon\tau$, is obtained by substitution of the fast equilibrium into the complete model. This reduced model reads as follows:

$$\begin{cases} \frac{\mathrm{d}n}{\mathrm{d}t} = \{\phi_1(n_1^*)n_1^* + \phi_2(n_2^*)n_2^*\} - \{\widetilde{\phi}_1(n_1^*)p_1^* + \widetilde{\phi}_2(n_2^*)p_2^*\} \\ \frac{\mathrm{d}p}{\mathrm{d}t} = -\{\psi_1(p_1^*) + \psi_2(p_2^*)\} + \{\widetilde{\psi}_1(n_1^*)p_1^* + \widetilde{\psi}_2(n_2^*)p_2^*\} \end{cases} \tag{9}$$

where n_i^*, p_i^* are all depending on n and p as given by (8).

We recall that to apply the method of aggregation of variables, [15,16], the following conditions have to be satisfied:

(1) The fast equilibrium has to be asymptotically stable for system (3).
(2) The parameter ε must be small enough ($\varepsilon \ll 1$).

In conclusion, when the hypothesis conditions are satisfied condition 1 holds.

3. Study of an example of predator–prey model with prey density-dependent migration of predators and predator density-dependent migration of prey

3.1. The complete model with density-dependent migrations

This section is devoted to the study of a particular model that reads as follows:

$$\begin{cases} \frac{dn_1}{d\tau} = (\alpha_2 p_2 + \alpha_0)n_2 - (\alpha_1 p_1 + \alpha_0)n_1 + \varepsilon\left[r_1 n_1\left(1 - \frac{n_1}{K_1}\right) - a_1 n_1 p_1\right] \\ \frac{dn_2}{d\tau} = (\alpha_1 p_1 + \alpha_0)n_1 - (\alpha_2 p_2 + \alpha_0)n_2 + \varepsilon\left[r_2 n_2\left(1 - \frac{n_2}{K_2}\right) - a_2 n_2 p_2\right] \\ \frac{dp_1}{d\tau} = \left(\frac{p_2}{\beta_2 n_2 + \beta_0} - \frac{p_1}{\beta_1 n_1 + \beta_0}\right) + \varepsilon[-\mu_1 p_1 + b_1 n_1 p_1] \\ \frac{dp_2}{d\tau} = \left(\frac{p_1}{\beta_1 n_1 + \beta_0} - \frac{p_2}{\beta_2 n_2 + \beta_0}\right) + \varepsilon[-\mu_2 p_2 + b_2 n_2 p_2] \end{cases} \tag{10}$$

We make a particular choice for functions f_i. We choose a linear affine dependence of prey migration rates with respect to local predator density, $f_1(p_1) = \alpha_1 p_1 + \alpha_0$ and $f_2(p_2) = \alpha_2 p_2 + \alpha_0$ where α_0, α_1 and α_2 are non-negative parameters. In absence of predators, prey move from one patch to the other at the same constant rate α_0. We also choose particular predator migration rates with respect to local prey density, $g_1(n_1) = \frac{1}{\beta_1 n_1 + \beta_0}$ and $g_2(n_2) = \frac{1}{\beta_2 n_2 + \beta_0}$, with β_0, β_1 and β_2 non-negative parameters. When there are no prey, predators move from patch to patch at the same constant rate, $1/\beta_0$.

Concerning local dynamics, we assume for prey a logistic growth on each patch with respective intrinsic growth rates, r_1 and r_2, and carrying capacities, K_1 and K_2; for predators, in absence of prey and we assume a natural mortality with constant per capita mortality rates, μ_1 and μ_2. Finally we use a Lotka–Volterra linear functional response on each patch with predation coefficients for prey, a_1 and a_2, and predation coefficients, b_1 and b_2, for predators. It is common supposing that $b_1 = ea_1$ and $b_2 = ea_2$ where $e \in]0,1[$ is a prey into predator biomass conversion parameter.

We will pursue the study of system (10) in two steps: first we give the explicit expression of the fast equilibrium and the associated aggregated model and then we present results of numerical bifurcation analysis of the aggregated model.

3.2. Fast equilibrium

To determine the fast equilibrium of (10), we suppose n and p positive constants and solve the following system:

$$\begin{cases} (\alpha_2 p_2 + \alpha_0)n_2 - (\alpha_1 p_1 + \alpha_0)n_1 = 0 \\ \frac{p_2}{\beta_2 n_2 + \beta_0} - \frac{p_1}{\beta_1 n_1 + \beta_0} = 0 \end{cases} \tag{11}$$

which is then equivalent to

$$\begin{cases} (\alpha_2(p - p_1) + \alpha_0)(n - n_1) = (\alpha_1 p_1 + \alpha_0)n_1 \\ (p - p_1)(\beta_1 n_1 + \beta_0) = p_1(\beta_2(n - n_1) + \beta_0) \end{cases} \tag{12}$$

Making $D = n_1 p_1$ system (12) can be transformed into

$$\begin{cases} (2\alpha_0 + \alpha_2 p)n_1 + (\alpha_2 n)p_1 = (\alpha_0 n + \alpha_2 np) + (\alpha_2 - \alpha_1)D \\ (\beta_1 p)n_1 - (2\beta_0 + \beta_2 n)p_1 = (\beta_1 - \beta_2)D - \beta_0 p \end{cases}$$

and using the following notations:

$$\Delta = \begin{vmatrix} (2\alpha_0 + \alpha_2 p) & (\alpha_2 n) \\ (\beta_1 p) & -(2\beta_0 + \beta_2 n) \end{vmatrix} = -(2\alpha_0 + \alpha_2 p)(2\beta_0 + \beta_2 n) - \alpha_2\beta_1 np$$

$$\Delta_{n_1} = \begin{vmatrix} (\alpha_0 n + \alpha_2 np) + (\alpha_2 - \alpha_1)D & (\alpha_2 n) \\ (\beta_1 - \beta_2)D - \beta_0 p & -(2\beta_0 + \beta_2 n) \end{vmatrix} = AD + B$$

$$\Delta_{p_1} = \begin{vmatrix} (2\alpha_0 + \alpha_2 p) & (\alpha_0 n + \alpha_2 np) + (\alpha_2 - \alpha_1)D \\ (\beta_1 p) & (\beta_1 - \beta_2)D - \beta_0 p \end{vmatrix} = CD + E$$

with

$$A = \alpha_2 n(\beta_2 - \beta_1) - (2\beta_0 + \beta_2 n)(\alpha_2 - \alpha_1)$$
$$B = \beta_0\alpha_2 np - (2\beta_0 + \beta_2 n)(\alpha_0 + \alpha_2 p)n$$
$$C = (2\alpha_0 + p\alpha_2)(\beta_1 - \beta_2) - \beta_1 p(\alpha_2 - \alpha_1)$$
$$E = -\beta_0 p(2\alpha_0 + p\alpha_2) - \beta_1 np(\alpha_0 + \alpha_2 p)$$

we can express the fast equilibrium as follows:

$$n_1^* = \frac{AD + B}{\Delta}, \quad p_1^* = \frac{CD + E}{\Delta}, \quad n_2^* = n - n_1^*, \quad p_2^* = p - p_1^* \tag{13}$$

where D is then the positive solution to

$$D = \left(\frac{AD + B}{\Delta}\right)\left(\frac{CD + E}{\Delta}\right)$$

or equivalently to the second order polynomial equation

$$(AC)D^2 + (AE + BC - \Delta^2)D + BE = 0$$

and thus

$$D = \frac{-(AE + BC - \Delta^2) - \sqrt{(AE + BC - \Delta^2)^2 - 4(AC)(BE)}}{2(AC)} \tag{14}$$

Two cases must be considered:

Case 1. $A = 0$ or $C = 0$:

the polynomial equation becomes $(AE + BC - \Delta^2)D + BE = 0$ which is equivalent to $D = (BE)/(AE + BE - \Delta^2)$.

Case 2. A and C are different from zero: then expression (14) holds.

As we have already seen in the general Section 2 concerning the fast system, this fast positive equilibrium is locally asymptotically stable for the fast dynamics. In what follows, we will use the method of aggregation of variables to determine the aggregated model. In our case, the fast equilibrium is asymptotically stable and assuming that parameter ε is small ($\varepsilon \ll 1$), the method of aggregation of variables can be applied.

3.3. Aggregated system

The aggregated model (9) for the particular model (10) reads as follows:

$$\begin{cases} \frac{dn}{dt} = r_1 n_1^* \left(1 - \frac{n_1^*}{K_1}\right) + r_2 (n - n_1^*)\left(1 - \frac{n - n_1^*}{K_2}\right) - (a_1 n_1^* p_1^* + a_2 (n - n_1^*)(p - p_1^*)) \\ \frac{dp}{dt} = -(\mu_1 p_1^* + \mu_2 (p - p_1^*)) + b_1 n_1^* p_1^* + b_2 (n - n_1^*)(p - p_1^*) \end{cases} \quad (15a, b)$$

where n_1^* and p_1^* are given by (13).

The structure of general aggregated model (15) is completely new with respect to both the local dynamics included in the initial model (10) and to classical models generally found in mathematical ecology literature. However, for particular values of parameters we recover some classical models.

Indeed, when we assume that $\alpha_0 = \beta_0 = 0$, a straightforward calculation shows that the fast equilibrium is proportional to the total density; that is $n_1^* = \theta n$ and $p_1^* = \overline{\theta} p$, where θ and $\overline{\theta}$ are constant and are expressed in terms of α_1, α_2, β_1 and β_2. A similar result also holds for the density independent migration case, i.e. when $\alpha_1 = \alpha_2 = 0$, $\beta_1 = \beta_2 = 0$ while $\alpha_0 \neq 0$ and $\beta_0 \neq 0$. In this last case, the fast equilibrium is simply the following one:

$$n_1^* = \frac{n}{2} \quad \text{and} \quad p_1^* = \frac{p}{2}$$

In both previous particular cases, the aggregated model (15) takes the next simple form corresponding to the classical model studied in [24,25]

$$\begin{cases} \frac{dn}{dt} = Rn\left(1 - \frac{n}{\tilde{K}}\right) - anp \\ \frac{dp}{dt} = -\mu p + bnp \end{cases}$$

where R, $\tilde{K}$, a, μ and b are positive parameters obtained in terms of the 'local' parameters of the complete model. The mathematical analysis (steady states and stability) can be found in the references cited above. We just recall that this classical model predicts:

- Predator extinction for a carrying capacity $\tilde{K}$ smaller than a certain threshold.
- Otherwise, predator–prey coexistence at a positive globally asymptotically stable equilibrium.

3.4. Analytical results of the general aggregated model

We shall now give some analytical results regarding the general aggregated model (15). First, we can observe that for $n = 0$ we have $n_1^* = n_2^* = 0$ and $p_1^* = p_2^* = p/2$ and, analogously, for $p = 0$ we have $n_1^* = n_2^* = n/2$ and $p_1^* = p_2^* = 0$. So, for system (15) we have that $(0,0)$ is an equilibrium $\{(0,p) \in \mathbb{R}^2 : p > 0\}$ and $\{(n,0) \in \mathbb{R}^2 : n > 0\}$ are invariant sets and, therefore, the interior of the positive quadrant $\mathrm{int}\mathbb{R}^2_+ = \{(n,p) \in \mathbb{R}^2 : n, p > 0\}$ is also an invariant set of the aggregated system. Moreover, we prove in the following lemma that solutions are bounded.

Lemma. *All solutions of system (15) in $\mathbb{R}^2_+$ are bounded.*

Proof. Let us define the function $W(t) = n(t) + p(t)$, then the time derivative of W along the solutions of system (15) is

$$\frac{dW}{dt} = r_1 n_1^* \left(1 - \frac{n_1^*}{K_1}\right) + r_2(n - n_1^*)\left(1 - \frac{n - n_1^*}{K_2}\right) - (\mu_1 p_1^* + \mu_2(p - p_1^*)) + (b_1 - a_1)n_1^* p_1^* + (b_2 - a_2)(n - n_1^*)(p - p_1^*)$$

Supposing $b_1 \leqslant a_1$ and $b_2 \leqslant a_2$, which is always possible by choosing the appropriate unities for prey and predator biomasses, then for each $\mu > 0$ the following inequality holds:

$$\frac{dW}{dt} + \mu W \leqslant r_1 n_1^* \left(\frac{\mu}{r_1} + 1 - \frac{n_1^*}{K_1}\right) + r_2(n - n_1^*)\left(\frac{\mu}{r_2} + 1 - \frac{n - n_1^*}{K_2}\right) + [\mu - \min(\mu_1, \mu_2)]p$$

if we now take $0 < \mu \leqslant \min(\mu_1, \mu_2)$, calling $M = \frac{r_1 K_1}{4}\left(\frac{\mu}{r_1} + 1\right)^2 + \frac{r_2 K_2}{4}\left(\frac{\mu}{r_2} + 1\right)^2$ and having in mind that $\max_{n_i^*}\left[r_i n_i^*\left(\frac{\mu}{r_i} + 1 - \frac{n_i^*}{K_i}\right)\right] = \frac{r_i K_i}{4}\left(\frac{\mu}{r_i} + 1\right)^2, i = 1, 2$, then we obtain that

$$\frac{dW}{dt} + \mu W \leqslant M$$

$$\frac{d}{dht}(e^{\mu t} W) = e^{\mu t}\frac{dW}{dt} + \mu e^{\mu t} W \leqslant M e^{\mu t}$$

and integrating between 0 and t we have

$$e^{\mu t} W(t) - W(0) \leqslant \frac{M}{\mu}(e^{\mu t} - 1)$$

$$W(t) \leqslant W(0)e^{-\mu t} + \frac{M}{\mu}(1 - e^{-\mu t})$$

which implies that $W(t) \leqslant \max\left(W(0), \frac{M}{\mu}\right)$ □

It is easy to show that the general aggregated model (15) has the following equilibria:

- A trivial equilibrium $E_0 = (0, 0)$.
- A predator free equilibrium $E_1 = (\bar{K}, 0)$, where $\bar{K} = \frac{2(r_1 + r_2)}{\left(\frac{r_1}{K_1} + \frac{r_2}{K_2}\right)}$.
- Possibly a positive predator–prey equilibrium $E^* = (n^*, p^*)$.

A straightforward calculation shows that the Jacobian matrix associated with E_0 has two eigenvalues $\lambda_1 = \frac{r_1 + r_2}{2}$ and $\lambda_2 = -\left(\frac{\mu_1 + \mu_2}{2}\right)$. Thus, E_0 is a saddle point.

For the axial equilibrium E_1, denoting $f(n,p)$ the right-hand side of (15a) and $g(n,p)$ of (15b), the Jacobian matrix of the aggregated system (15) evaluated at it verifies that

$$\frac{\partial g}{\partial n}(\bar{K}, 0) = 0$$

and, therefore, its eigenvalues are the diagonal elements $\frac{\partial f}{\partial n}(\bar{K}, 0)$ and $\frac{\partial g}{\partial p}(\bar{K}, 0)$. After some calculations, including implicit derivation in equalities (12), we found that

$$\frac{\partial f}{\partial n}(\bar{K},0) = -\frac{r_1 + r_2}{2}$$

and

$$\frac{\partial g}{\partial p}(\bar{K},0) = (\beta_1\bar{K} + \beta_2\bar{K} + 4\beta_0)\left[-\left(\mu_1 + \mu_2 + b_2\frac{\bar{K}}{2} - b_1\frac{\bar{K}}{2}\right)(\beta_1\bar{K} + 2\beta_0) + \left(b_2\frac{\bar{K}}{2} - \mu_2\right)(\beta_1\bar{K} + \beta_2\bar{K} + 4\beta_0)\right]$$

Having in mind that $(\beta_1\bar{K} + \beta_2\bar{K} + 4\beta_0) > 0$ the stability of $E_1(\bar{K},0)$ depends on the following quantity:

$$q = -\left(\mu_1 + \mu_2 + b_2\frac{\bar{K}}{2} - b_1\frac{\bar{K}}{2}\right)(\beta_1\bar{K} + 2\beta_0) + \left(b_2\frac{\bar{K}}{2} - \mu_2\right)(\beta_1\bar{K} + \beta_2\bar{K} + 4\beta_0)$$

as follows:

- $E_1(\bar{K},0)$ is stable if $q < 0$,
- $E_1(\bar{K},0)$ is unstable if $q > 0$.

We can remark that q is positive, and therefore E_1 is unstable, for large values of $\bar{K}$.

Existence, uniqueness and stability of the positive equilibrium E^* are checked numerically by bifurcation analysis in the next section.

3.5. Numerical bifurcation analysis

3.5.1. Numerical bifurcation analysis of the aggregated model

This section is devoted to the numerical bifurcation analysis of the aggregated model (15). We present bifurcation diagrams for the aggregated model. The bifurcation diagrams were calculated using the software packages AUTO [26], LOCBIF [27,28] and Maple [29]. Fig. 1 is a two-parameter bifurcation diagram where β_2/β_0 and $K = K_1 = K_2$ act as bifurcation parameters.

The fixed parameter values are given in Table 1. Below the transcritical bifurcation TC at a low carrying capacity K, only the prey populations exist in the two patches, in equilibrium $E_1 = (K,0)$. Above the TC curve, the positive equilibrium $E^* = (n^*,p^*)$ exists.

For fixed $K = 60$, there is one supercritical Hopf bifurcation H^- for small values of the ratio β_2/β_0 and one subcritical Hopf bifurcation H^+ for high values of the ratio. There is an intermediate critical point $(K,\beta_2/\beta_0)$ where the Hopf bifurcation changes nature. The critical point is a codim two Bautin bifurcation point. This point is denoted by B in the two-parameter bifurcation diagram in Fig. 1. The tangent bifurcation of the limit cycle, denoted by T_c originates in this point.

In a one-parameter bifurcation diagram in Fig. 2 the biomass of the prey, n, (bottom panel) and predator, p, (top panel) are plotted as a function of the free parameter β_2/β_0 while other parameters are fixed at values given, while $K = 60$. Stable equilibria are presented by a solid line and unstable equilibria by a dashed line in which case there is a limit cycle that surrounds the unstable equilibrium. The maximum and minimum values during one period are plotted as solid lines when the limit cycle is stable and dashed lines when it is unstable.

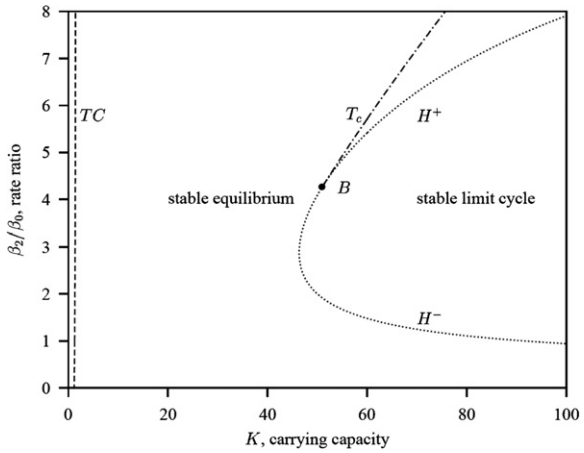

Fig. 1. The two-dimensional bifurcation diagram for the aggregated system using β_2/β_0 and K (where $K = K_1 = K_2$) as bifurcation parameters. Supercritical Hopf bifurcation (H^-) and sub critical Hopf bifurcation (H^+) mark regions on the right-hand side where the system cycles. On the right-hand side of the transcritical (TC) bifurcation curve there is a positive equilibrium. Parameters: free parameters are β_2 and K. Fixed parameters values are given in Table 1.

Table 1
Parameter values for bifurcation analysis

Parameters	Notation	Value
Prey growth rate ($r_1 = r_2$)	r	0.6
Prey capture coefficient on patch 1	a_1	0.6
Prey capture coefficient on patch 2	a_2	0.3
Predator mortality rate ($\mu_1 = \mu_2 = \mu$)	μ	0.3
Predator predation coefficient on patch 1	b_1	0.3
Predator predation coefficient on patch 2	b_2	0.2
Prey density-dependent parameter for predator migration on patch 1	β_1	2.792403
Prey density-dependent parameter for predator migration on patch 2	β_2	Bifurcation parameter
Inverse of predator migration rate when the prey density is equal to zero	β_0	10
Predator density-dependent parameter for prey migration on patch 1	α_1	2
Predator density-dependent parameter for prey migration on patch 2	α_2	1
Prey migration rate when the predator density is equal to zero	α_0	10
Prey carrying capacity ($K_1 = K_2 = K$)	K	Bifurcation parameter

The system shows a stable equilibrium for ratio-values below H^- and above H^+. Between these two Hopf bifurcations there is an unstable equilibrium. In the region between H^+ and the tangent bifurcation for the limit cycle T_c the stable equilibrium coexists with a stable limit cycle. The separatrix is formed by the stable manifold of the saddle limit cycle. The stable and saddle limit cycle collide and disappear at the tangent bifurcation T_c.

3.5.2. Numerical bifurcation analysis of the complete model

The bifurcation diagrams for the full model with $\varepsilon = 0.01$ are shown in Figs. 3 and 4. The overall picture of the diagrams is the same as for the aggregated model, however in the two parameter

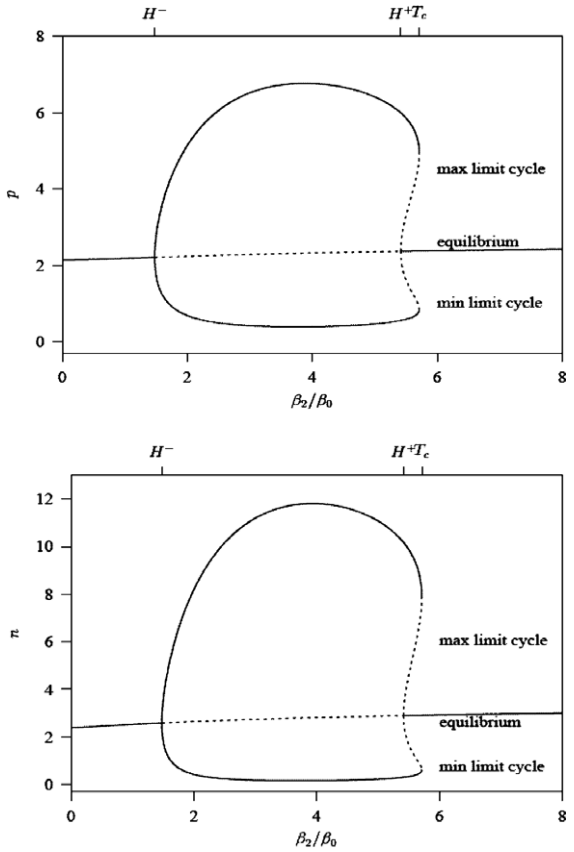

Fig. 2. One-parameter diagram of the prey (bottom) predator (top) biomasses, n and p, respectively, with ratio β_2/β_0 as bifurcation parameter and $K = 60$. This point is above the Bautin bifurcation point B where the positive equilibrium becomes unstable at a supercritical Hopf bifurcation H^-, where stable oscillations occur. For these limit cycles the maximum and minimum values are plotted. Parameters as in Fig. 1.

diagrams, the transcritical bifurcation curve remains at about the same position while the Hopf bifurcation curve moves to the right when ε increases. Thus the system with more equal time scales appears to be stable in a larger part of the diagram.

3.6. Two previous cases revisited

In two previous papers, we studied the two processes independently:

- Predator density-dependent migration of prey, $\alpha_1 = \alpha_2 = 0$, Mchich et al. [2].
- Prey density-dependent migration of predators, $\beta_1 = \beta_2 = 0$ and $K_1 = K_2 \to \infty$, Mchich et al. [3].

We shall now use our results to revisit the two special cases studied in these previous articles.

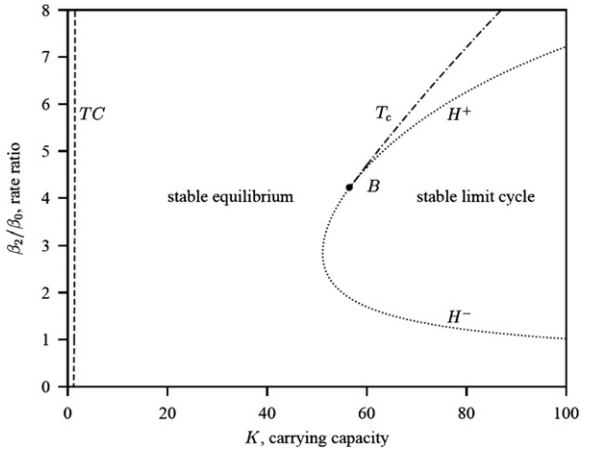

Fig. 3. The two-dimensional bifurcation diagram for the complete system using β_2/β_0 and K as bifurcation parameters for $\varepsilon = 0.01$. Supercritical Hopf bifurcation (H^-) and sub critical Hopf bifurcation (H^+) mark regions on the right-hand side where the system cycles. On the right-hand side of the transcritical (TC) bifurcation curve there is a positive equilibrium. Parameters: free parameters are β_2 and K. Fixed parameters values are given in Table 1.

3.6.1. Special case 1 revisited: $\alpha_1 = \alpha_2 = 0$

In [2], was analysed the case where $\alpha_1 = \alpha_2 = 0$. Substitution of these values in system (10) gives the following equilibrium for the fast system:

$$n_1^* = \frac{n}{2} \quad \text{and} \quad p_1^* = \frac{(\beta_1 n + 2\beta_0)p}{(\beta_1 + \beta_2)n + 4\beta_0}$$

A two-parameter bifurcation diagram, with the same conditions to that in Fig. 1, is shown in Fig. 5 for this particular case $\alpha_1 = \alpha_2 = 0$. There is no Bautin point so there are two regions. For low K-values only the prey population is present. For higher K-values there is coexistence of the prey and predator populations. Between the curves T_c and H^- the system possesses a stable equilibrium and on the right-hand side of H^- there is a stable limit cycle within a window of ratio β_2/β_0.

3.6.2. Special case 2 revisited: $\beta_1 = \beta_2 = 0$ and $K_1 = K_2 \to \infty$

In [3], a special case was analysed with $\beta_1 = \beta_2 = 0$ and $K_1 = K_2 \to \infty$. Substitution of these values in our general model leads to the following equilibrium for the fast system:

$$n_1^* = \frac{(\alpha_2 p + 2\alpha_0)n}{(\alpha_1 + \alpha_2)p + 4\alpha_0} \quad \text{and} \quad p_1^* = \frac{p}{2}$$

and the following aggregated model:

$$\begin{cases} \frac{dn}{dt} = r_1 n_1^* + r_2(n - n_1^*) - (a_1 n_1^* + a_2(n - n_1^*))\frac{p}{2} \\ \frac{dp}{dt} = (-(\mu_1 + \mu_2) + b_1 n_1^* + b_2(n - n_1^*))\frac{p}{2} \end{cases}$$

For the numerical values chosen in Table 1 (for r_1, r_2, a_1, a_2, μ_1, μ_2, b_1, b_2, β_0, α_0 and α_1) and taking as bifurcation parameter α_2, a critical point occurs at $\alpha_2 = 2$. Here, the real part of the eigenvalues

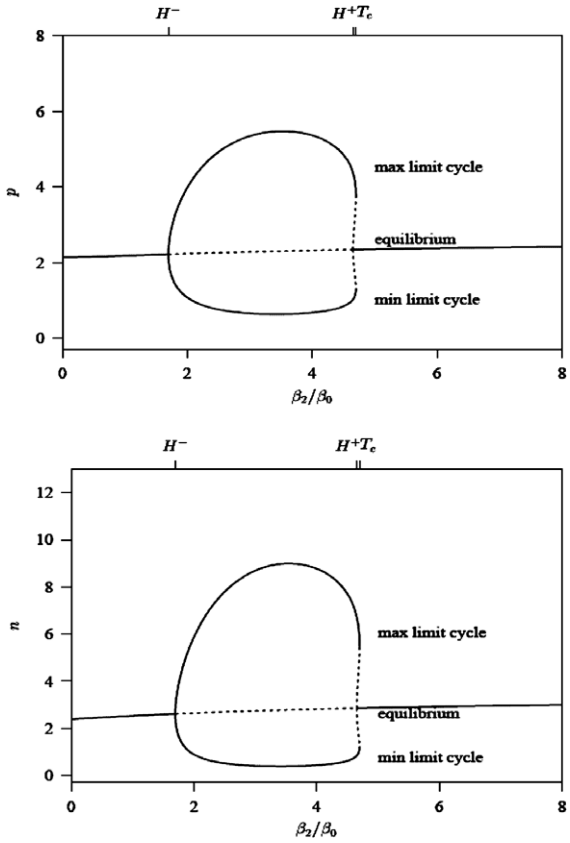

Fig. 4. One-parameter diagram of the prey (bottom) predator (top) biomasses, n and p, respectively, from the complete model with ratio β_2/β_0 as bifurcation parameter and $K = 60$ with $\varepsilon = 0.01$. This point is above the Bautin bifurcation point B where the positive equilibrium becomes unstable at a supercritical Hopf H^-, where stable oscillations occur. For these limit cycles the maximum and minimum values are plotted. Parameters as in Fig. 3.

of the Jacobian matrix at the positive equilibrium $E^* = (n^*, p^*)$ is zero, indicating a change in the long-term dynamics when the parameter is varied. In [3] the criterion for a Hopf bifurcation (the trace of the Jacobian matrix has to be zero) is worked out. The derived test-function reads

$$\alpha_2 b_1 + \alpha_1 b_2 = \alpha_1 b_1 + \alpha_2 b_2$$

They show that the equilibrium point at the critical parameter value is a centre. In the phase portrait the trajectories are closed curves around the unstable equilibrium point. These trajectories are neutral stable orbits, like in the classical Lotka–Volterra model. For $\alpha_2 < 2$, the aggregated model for the reference parameters except $K_1 = K_2 \to \infty$ and $\beta_1 = \beta_2 = 0$ the system is stable and for $\alpha_2 > 2$ it is unstable. When the equilibrium is unstable, by the use of the negative Dulac's criterion it is shown that the aggregated model cannot have closed orbits and that the predator–prey system is not persistent.

Here we perform a normal form analysis of this critical point. We follow the procedure described in [28] closely. The planar system is written as

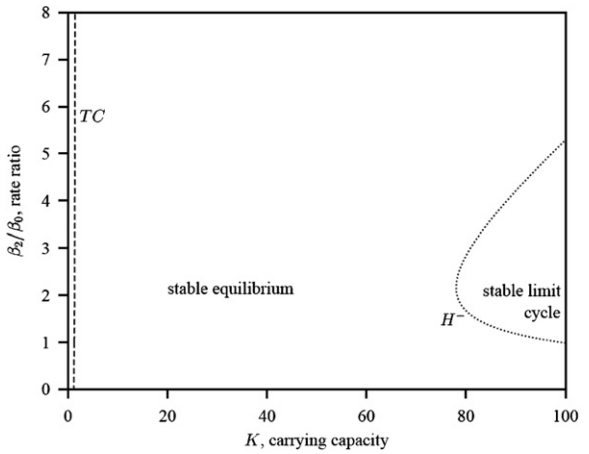

Fig. 5. The two-dimensional bifurcation diagram for the system analysed in [1] using β_2/β_0 and K as bifurcation parameters. Supercritical Hopf bifurcation (H^-). Parameters: free parameters are β_2 and K. Fixed parameters values are given in Table 1.

$$\frac{\mathrm{d}x}{\mathrm{d}t} = J(\alpha)x + F(x,\alpha)$$

where $x \in \mathbb{R}^2$, parameter $\alpha \in \mathbb{R}$, J is again the Jacobian matrix and $F(x,\alpha)$ is a smooth function representing the non-linear terms.

First the system is written in a coordinate system where the equilibrium is shifted to the origin of the phase plane by a coordinate transformation and also the bifurcation parameter α, is translated such that the critical point is at zero. Second, the planar system is written in a single ODE for the complex variable $z \in \mathrm{C}$. Furthermore, using the eigenvector p and adjoint eigenvector q of the Jacobian matrix evaluated at the equilibrium, the linear part is transformed in the simplest form. The result is

$$\frac{\mathrm{d}z}{\mathrm{d}t} = \lambda(\alpha)z + g(z,\bar{z},\alpha)$$

where λ is the complex eigenvalue of the Jacobian matrix and g the complex valued function which describes the non-linear terms. At the Hopf bifurcation for $\alpha = 0$ we have $\lambda_{1,2} = \mathrm{i}\omega_0$ where $\omega_0 > 0$. This function is replaced by its formal Taylor series in the two complex variables z and $\bar{z}$

$$\frac{\mathrm{d}z}{\mathrm{d}t} = \lambda(\alpha)z + \sum_{k+l\geqslant 2} \frac{1}{k!l!} g_{kl}(\alpha) z^k \bar{z}^l \tag{16}$$

where

$$g_{kl}(\alpha) = \frac{\partial^{k+l}}{\partial z^k \partial \bar{z}^l} \langle p(\alpha), F(zq + \bar{z}\bar{q}, \alpha)\rangle|_{z=0} \tag{17}$$

Third, this expression is simplified by a non-linear (complex) coordinate change by removing all quadratic terms. Thereafter, in a similar manner, it is tried to eliminate the cubic terms. In general, only one cubic term remains and this leads to the equation with only one cubic term denoted by complex c_1 that is proportional to the first [28, Definition 3.3] Lyapunov coefficient $l_1(\alpha)$. The equation reads

$$\frac{dz}{dt} = \lambda(\alpha)z + c_1(\alpha)z^2\bar{z} + O(|z|^4)$$

An expression of the real first Lyapunov coefficient $l_1(0) = \mathrm{Re}(c_1(0))/\omega_0$ evaluated at the critical point in the third-order terms is given in [28, Eq. (3.20)].

$$l_1(0) = \frac{1}{2\omega_0^2}\mathrm{Re}(ig_{20}g_{11} + \omega_0 g_{21})$$

Calculations using [29] revealed that this coefficient is zero and therefore the Hopf bifurcation is degenerated and called a Bautin bifurcation point.

Because all cubic terms can be eliminated we continue with higher order terms. It appears to be possible to eliminate all quadric terms without changing the cubic terms so the next interesting terms are the fifth-order terms. Similar to the third-order terms only one fifth-order term remains and this term is proportional to the complex coefficient $c_2(\alpha)$.

$$\frac{dz}{dt} = \lambda(\alpha)z + c_1(\alpha)z^2\bar{z} + c_2(\alpha)z^3\bar{z}^2 + O(|z|^6)$$

The real second Lyapunov coefficient $l_2(\alpha)$ is defined in [28, Definition 8.1] and an expression of this coefficient is given in [28, Eq. (8.23)] expressed in the Taylor series expansion coefficients in (16) evaluated at the critical point $\alpha = 0$ where $l_2(0) = \mathrm{Re}(c_2(0))/\omega_0$. Also this Lyapunov coefficient is, however, zero. Hence the two coefficients in the Poincaré normal form for the Bautin point are both zero at the critical point. In conclusion, the bifurcation point is a degenerated Bautin point. This explains the phenomenon described in [3] where a centre for the equilibrium was found at the Hopf bifurcation.

To illustrate the link between analysis in [3] and the normal form analysis we consider the expression obtained after the linear transformation, Eqs. (16) and (17). It appears to be of the form

$$\frac{dz}{dt} = i\omega z + (a + ib)(\bar{z}^2 - z^2)$$

where $\omega, a, b \in \mathbb{R}$. Notice that there are no higher order terms. When we write $z = x + iy$ this system is equivalent with

$$\frac{dx}{dt} = -\omega y + 4bxy$$
$$\frac{dy}{dt} = \omega x - 4axy$$

This is a special case of the classical Lotka–Volterra model where the birth rate of the prey equals just the death rate of the predator. This result is in agreement with the simulation results given in [3, Fig. 3]. The calculated trajectories are the well-known closed trajectories around the unstable equilibrium. The periodic solution is neutral stable. This analysis shows also why there does not need to be a tangent bifurcation curve for limit cycles originating from this point. For, with the analysis of the normal form of the Bautin point it is required that beside a zero first Lyapunov coefficient, the second Lyapunov coefficient is unequal zero.

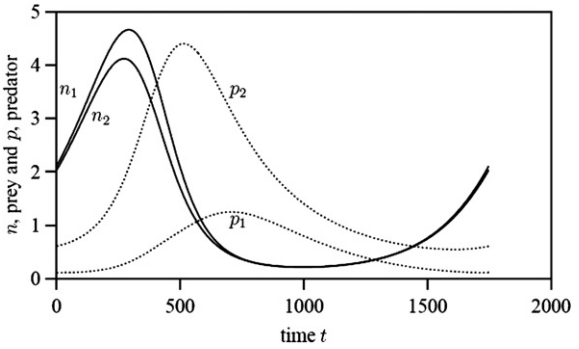

Fig. 6. Limit cycle oscillations of patch prey and predator densities with time of the full model where $\beta_2/\beta_0 = 0.4$, $\varepsilon = 0.01$ and $K = 60$. see Figs. 3 and 4. The period was 1749 time units.

We conclude from this that for the aggregated system besides the Hopf bifurcation, there needs to be no tangent bifurcation curve for limit cycles on the lower branch for small values of β_1 and β_2 and large values for K. In Fig. 6, the one-parameter bifurcation diagram is shown for the full model discussed in [3] for three values of the parameter ε.

4. Discussion and conclusions

To start we would like to stress a methodological point. Looking at Figs. 1 and 3 we observe that they are consistent. This means that the bifurcation diagrams obtained for the aggregated and complete models are almost similar for $\varepsilon = 0.01$. This result shows that the aggregated model can be used for bifurcation analysis instead of the complete model as soon as ε is small enough. Our numerical simulations show that it is not needed to consider a very small value for parameter ε. This is an interesting point because, in general, the complete model may involve a large set of variables and parameters, and it may be difficult to handle. Consequently, it may be advantageous to use the aggregated model with fewer variables and compound parameters to perform a numerical bifurcation analysis of the system even if the fast time scale and the slow time scale are not so different.

In [30–34], the within patch predator–prey system is described by the classical Lotka–Volterra model and constant per capita dispersal rates from each patch. Various adapted versions have been studied for the within patch dynamics, different prey birth [32] and delayed dispersal rates [33].

Returning to the main goal of this work, the study of the effects of density-dependent migrations on the dynamics of the predator–prey system with migrations acting at a faster scale than predator–prey interactions, let us first recall that in the density independent migration case, which corresponds to particular values of some of the parameters, namely $\alpha_1 = \alpha_2 = 0$ and $\beta_1 = \beta_2 = 0$ with $\alpha_0 \neq 0$ and $\beta_0 \neq 0$, the general aggregated model (15) reduces to a classical model. As mentioned above, in this case, when the positive equilibrium E^* exists, it is always stable. This stability property is found for any value of K, the prey carrying capacity in the aggregated system. In other

words, in the density independent case, there is no 'paradox of enrichment' and asymptotically, prey and predator coexist at constant densities.

On the contrary, in the general density-dependent case, our results show that, for some values of the ratio β_2/β_0 and when the carrying capacity of the prey K increases, the positive equilibrium E^* looses its stability via a supercritical Hopf bifurcation with appearance of a stable limit cycle. Figs. 2 and 4 show amplitudes of total prey and predator densities along the limit cycle that occurs in a given window of the ratio β_2/β_0. We also observe that, if we assume a maximum value for the prey carrying capacity, the equilibrium E^* is always stable for small as well as large ratio β_2/β_0, see Figs. 2 and 4.

The within patch dynamics in our model is described by the generalized Lotka–Volterra model with always a stable positive equilibrium when it exists. So, only destabilizing effects by dispersal can be observed. Under the conditions mentioned above, the predator density dependence of prey migration coupled to the prey density-dependent predator migration destabilizes the predator–prey equilibrium E^* under enriched conditions (large K). However, the predator prey system still remains persistent and we observe cyclic variations of total prey and predator densities according to a limit cycle. Local patch densities are linked to total densities through complex fast

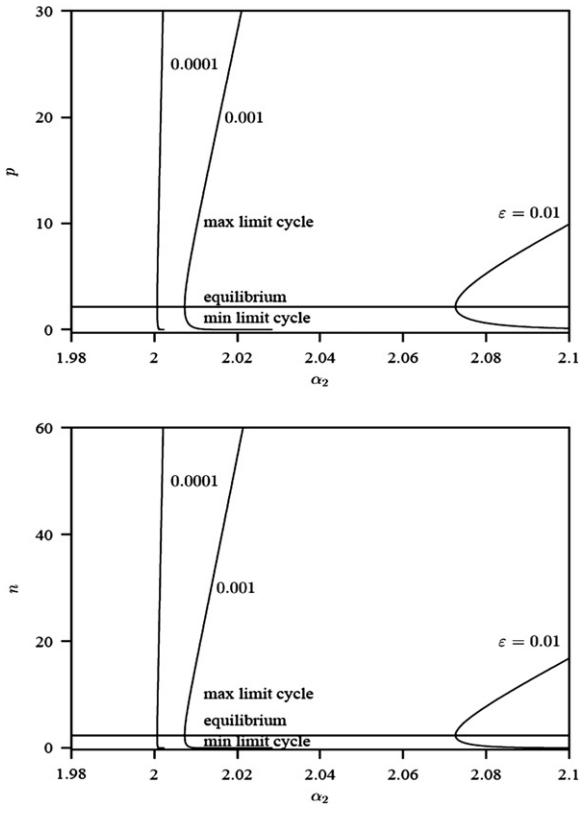

Fig. 7. One-parameter diagram of the prey (bottom) predator (top) biomasses, n and p, respectively, for the special case $K_1 = K_2 = \infty$ and $\beta_1 = \beta_2 = 0$ discussed in [2]. The full model is analysed with α_2 as bifurcation parameter for three values of ε, namely 0.01, 0.001, 0.0001. In the aggregated model for $\alpha_2 = 2$ the equilibrium is a centre.

equilibrium expressions (13). Fig. 6 shows periodic oscillations of prey and predator patch densities along the stable limit cycle which are almost in phase. This is an interesting point which shows that fast migration between patches can result in synchronized oscillations and this result could probably be extended to a system of N patches ($N > 2$).

In the limiting case $K_1 = K_2 \to \infty$, the generalized Lotka–Volterra model becomes the classical Lotka–Volterra model that produces neutrally stable oscillations in which the amplitude of the fluctuations depends on the initial conditions. From Fig. 7 we learn that there is a stabilizing effect in a region of the α_1, α_2 parameter space bounded by a Hopf bifurcation. In the case of fast emigration rates where $\varepsilon = 0$, either there is stabilization or the system explodes depending on the α_1, α_2 parameter values and these two regions are separated by a degenerated Bautin point analysed in Section 3.6.2.

We must also note that the equilibrium total prey and predator densities (or the average densities for limit cycle), slightly increases as the ratio β_2/β_0 also increases, see Figs. 2 and 4. This result shows that the density dependence of migrations has a positive effect on the total equilibrium densities for prey as well as for predators.

Figs. 1 and 3 also show that in a small range of values of ratio β_2/β_0, there is coexistence of a stable and unstable limit cycle. This kind of situations is rather unusual for predator–prey models and results from the density dependence of prey and predator migrations. Such a case was also obtained in a previous predator–prey model [23].

Acknowledgments

This work was partially supported by Ministerio de Educación y Ciencia (Spain), proyecto MTM2005-00423, and FEDER (P. Auger and R. Bravo de la Parra).

References

[1] C.J. Briggs, M.F. Hoopes, Stabilizing effects in spatial parasitoid – host and predator–prey models: a review, Theor. Popul. Biol. 65 (2004) 299.
[2] R. Mchich, P. Auger, R. Bravo de la Parra, N. Raissi, Dynamics of a fishery on two fishing zones with fish stock dependent migrations: aggregation and control, Ecol. Model. 158 (2002) 51.
[3] R. Mchich, P. Auger, J.C. Poggiale, Effect of predator density dependent dispersal of prey on stability of a predator–prey system, Math. Biosci. 206 (2007) 343.
[4] D. Tilman, P. Kareiva, Spatial Ecology, Princenton University Press, 1997.
[5] D.R. French, J.M.J. Travis, Density-dependent dispersal in host-parasitoid assemblages, Oikos 95 (2001) 125.
[6] P. Amarasekare, Interactions between local dynamics and dispersal: insights from single species models, Theor. Popul. Biol. 53 (1998) 44.
[7] I.M. Jánosi, I. Scheuring, On the evolution of density dependent dispersal in a spatially structured population model, J. Theor. Biol. 187 (1997) 397.
[8] B.E. Saether, S. Engen, R. Lande, Finite metapopulation models with density-dependent migration and stochastic local dynamics, Proc. R. Soc. Lond. B 266 (1999) 113.
[9] J.A.L. Silva, M.L. de Castro, D.A.R. Justo, Stability in a metapopulation model with density-dependent dispersal, Bull. Math. Biol. 63 (2001) 485.
[10] P. Amarasekare, Spatial variation and density-dependent dispersal in competitive coexistence, Proc. R. Soc. Lond. B 271 (2004) 1497.

[11] P. Amarasekare, The role of density-dependent dispersal in source–sink dynamics, J. Theor. Biol. 226 (2004) 159.
[12] N. Shigesada, J. Roughgarden, The role of rapid dispersal in the population dynamics of competition, Theor. Popul. Biol. 21 (1982) 353.
[13] Y. Iwasa, V. Andreasen, S.A. Levin, Aggregation in model ecosystems I. Perfect aggregation, Ecol. Model. 37 (1987) 287.
[14] Y. Iwasa, S.A. Levin, V. Andreasen, Aggregation in model ecosystems II. Approximate aggregation, IMA. J. Math. Appl. Med. Bio. 6 (1989) 1.
[15] P. Auger, R. Roussarie, Complex ecological models with simple dynamics: from individuals to populations, Acta Biotheor. 42 (1994) 111.
[16] P. Auger, J.C. Poggiale, Aggregation and emergence in systems of ordinary differential equations, in: P. Antonelli, P. Auger (Eds.), Special Issue: Aggregation and Emergence in Population Dynamics, Math. Comput. Model. 27 (1998) 1.
[17] P. Auger, R. Bravo de la Parra, Methods of aggregation of variables in population dynamics, CR Acad. Sci. Sci. de la Vie 323 (2000) 665.
[18] P. Auger, R. Bravo de la Parra, J.C. Poggiale, E. Sánchez, T. Nguyen Huu, Aggregation of variables and applications to population dynamics, Springer, 2007, Book chapter.
[19] P. Auger, D. Pontier, Fast game theory coupled to slow population dynamics: the case of domestic cat populations, Math. Biosci. 148 (1998) 65.
[20] A. Chaumot, S. Charles, P. Flammarion, J. Garric, P. Auger, Using aggregation methods to assess toxicant effects on population dynamics in spatial systems, Ecol. Appl. 12 (2002) 1771.
[21] C. Lett, P. Auger, R. Bravo de la Parra, Migration frequency and the persistence of host parasitoid interactions, J. Theor. Biol. 221 (2003) 639.
[22] E. Dubreuil, P. Auger, J.-M. Gaillard, M. Khaladi, Effects of aggressive behaviour on age structured population dynamics, Ecol. Model. 193 (2006) 777.
[23] P. Auger, B.W. Kooi, R. Bravo de la Parra, J.-C. Poggiale, Bifurcation analysis of a predator–prey model with predators using hawk and dove tactics, J. Theor. Biol. 238 (2006) 597.
[24] A.D. Bazykin, Nonlinear dynamics of interacting populations, World Scientific Ser. Nonlinear Sci. A 11 (1998).
[25] J.D. Murray, *Mathematical Biology*. Biomathematics text 19, Springer, Berlin, 1989.
[26] E.J. Doedel, A.R. Champneys, T.F. Fairgrieve, Y.A. Kuznetsov, B. Sandstede, X. Wang, Auto 97: Continuation and bifurcation software for ordinary differential equations, Technical Report, Concordia University, Montreal, Canada, 1997.
[27] A.I. Khibnik, Yu.A. Kuznetsov, V.V. Levitin, E.V. Nikolaev, Continuation techniques and interactive software for bifurcation analysis of ODEs and iterated maps, Physica D 62 (1993) 360.
[28] Yu. A. Kuznetsov, Elements of applied bifurcation theory, Applied Mathematical Sciences, third ed., vol. 112, Springer, New York, 2004.
[29] Maplesoft, Waterloo, Ontario, Canada, Maple software.
[30] S.A. Levin, Dispersal and population interactions A, Nature 108 (1974) 207.
[31] V.A.A. Jansen, Regulation of predator–prey systems trough spatial interactions: a possible solution to the paradox of enrichment, Oikos 74 (1995) 384.
[32] W.W. Murdoch, C.J. Briggs, R.M. Nisbet, Consumer-Resource Dynamics, Princeton University Press, Princeton, NJ, 2003.
[33] M.G. Neubert, P. Klepac, P. van der Driessche, Stabilizing dispersal delays in predator–prey metapopulation models, Theor. Popul. Biol. 61 (2002) 339.
[34] R.M. Nisbet, C.J. Briggs, W.S.C. Gurney, W.W. Murdoch, A. Stewart-Oaten, Two-patch metapopulation dynamics, in: S.A. Levin, J.H. Steele, T.M. Powell (Eds.), Patch Dynamics in Terrestrial, Freshwater, and Marine Ecosystems, Springer, Berlin, 1993.